

A family of three maximally symmetric boost-invariant flows in relativistic hydrodynamics

Sašo Grozdanov^{a,b}

^a*Higgs Centre for Theoretical Physics, School of Physics and Astronomy, University of Edinburgh, Edinburgh, EH8 9YL, Scotland*

^b*Faculty of Mathematics and Physics, University of Ljubljana, Jadranska ulica 19, SI-1000 Ljubljana, Slovenia*

ABSTRACT: I discuss the constructions of boost-invariant dissipative conformal hydrodynamic flows by elaborating on the geometric procedure by Gubser and Yarom, which starts from a static, maximally symmetric flow on $dS_3 \times \mathbb{R}$. Three foliations of dS_3 preserve three-dimensional non-Abelian isometry groups, namely, the flat $ISO(2)$ -invariant, the spherical (closed) $SO(3)$ -invariant, and the hyperbolic (open) $SO(2,1)$ -invariant slicings. I show that the fluids that preserve these symmetries, after they have been Weyl transformed to flat spacetime, give rise to three physically distinct and boost-invariant solutions of the relativistic dissipative Navier-Stokes equations: the well-known and widely studied Bjorken and Gubser flows, and a seemingly thus far unexplored solution that arises from the hyperbolic slicing of dS_3 . The new solution combines the radial expansion characteristic of the Gubser flow with the late-proper-time applicability of Bjorken's solution, and features a finite, radially bounded droplet whose expanding edge resembles a free-streaming shockwave.

Contents

1	Introduction	1
2	Construction of the three boost-invariant flows	2
2.1	Ideal hydrodynamic solutions in the auxiliary ($dS_3 \times \mathbb{R}$) space	2
2.2	Ideal hydrodynamic solutions in the physical (Minkowski) space	3
2.3	Viscous corrections	4
3	Discussion of the flow solutions and future directions	5

1 Introduction

Exact analytic solutions of non-linear partial differential equations are rare. This is especially true if the said solutions are meant to model interesting physical processes. The Navier-Stokes equations that describe the dynamics of dissipative fluids are no exception. These equations, which express the near-equilibrium evolution of long-lived conserved quantities, such as energy and momentum, have for over two centuries been successfully applied to an incredible array of phenomena in gases and liquids (see e.g. Refs. [1–3]). What may seem more surprising is that these equations in their relativistic form also describe certain phenomena in high-energy particle physics. In particular, they have been successfully applied to the description of heavy-ion collisions and the evolution of the quark-gluon plasma (QGP) (see Ref. [4]). Even though such phenomena occur at energies above a few TeV per nucleon pair (e.g., $\sqrt{s_{NN}} \sim 2.8\text{--}5.0$ TeV at the LHC) and the size of a typical QGP droplet is only of order a few femtometers ($\sim 5\text{--}10$ fm), due to the strong interactions of quantum chromodynamics (QCD), such states hydrodynamise in a remarkably short time (see Refs. [5–8]).

It was in 1982 that Bjorken found an exact $4d$ boost-invariant solution of relativistic and conformal Navier-Stokes equations [9]. This solution has been used extensively in modeling of high-energy flows, and has been applied to the physics of heavy ions. It enjoys the following set of symmetries: $SO(1,1) \times ISO(2) \times \mathbb{Z}_2$. Respectively, they correspond to boost invariance along the beam, translations and rotations in the transverse plane (i.e., the isometries of the $2d$ Euclidean plane) and reflection symmetry along the beam.

Another boost-invariant conformal solution was later found by Gubser in 2010 [10]. Its symmetry algebra has the same number of dimensions and is given by $SO(1,1) \times SO(3) \times \mathbb{Z}_2$, where $SO(3)$ is a subgroup of the conformal group $SO(4,2)$. This group structure was elucidated from a geometric point of view by Gubser and Yarom in Ref. [11].¹ While the

¹This method as well as other methods have been used to find other exact solutions, including some with rotation and some that include effects from second-order hydrodynamics [12–17].

Bjorken flow is translationally invariant in the transverse plane, the main advantage of the Gubser flow is its expanding radial profile.

In this note, I reexamine the symmetry structure of the Bjorken and Gubser solutions, and show that another, third solution exists in the same class of conformal boost-invariant flows with the same number of symmetry generators. Namely, instead of ISO(2) or SO(3), a fluid can be invariant under SO(2,1). In the geometric picture, these three symmetry groups correspond to the flat, closed spherical, and open hyperbolic slicings of the auxiliary 3d de Sitter space used in the construction by Ref. [11]. From this point of view, the Gubser flow is not a generalisation of the Bjorken flow. Both of those solutions, as well as the new one presented here, should be seen as three equivalent members of the same ‘maximally symmetric’ family of viscous boost-invariant solutions of the relativistic dissipative Navier-Stokes equations.

2 Construction of the three boost-invariant flows

I begin by constructing the boost-invariant flows with ‘maximal’ symmetry from a single, unified procedure that follows that of Gubser and Yarom [11]. The main strength of the approach was in providing a clear geometric understanding of the symmetries that underlie Gubser’s solution [10] known as the Gubser flow. Here, I show that there exist three such solutions, which are all symmetric under non-trivial symmetry algebras with the same dimension.

2.1 Ideal hydrodynamic solutions in the auxiliary ($dS_3 \times \mathbb{R}$) space

Consider an ideal conformal relativistic fluid in the $dS_3 \times \mathbb{R}$ geometry, where dS_3 is the three-dimensional de Sitter space. This manifold can be obtained as a Weyl transformation of the flat Minkowski space.² There are three ways in which dS_3 can be foliated with $2d$ slices that preserve the maximal amount of symmetries, namely, a three-dimensional algebra. These are the flat ($\kappa = 0$), the spherical ($\kappa = +1$) and the hyperbolic ($\kappa = -1$) slicings. In compact notation, setting the dS_3 radius to one, we can write the metric of $dS_3 \times \mathbb{R}$ as

$$d\hat{s}_\kappa^2 = -d\rho^2 + S_\kappa^2(\rho) (d\theta^2 + Q_\kappa^2(\theta)d\phi^2) + d\eta^2, \quad (2.1)$$

where (ρ, θ, ϕ) parametrise dS_3 and $\eta \in (-\infty, \infty)$ parametrises \mathbb{R} . In the three cases,

$$\kappa = 0 : \quad S_0(\rho) = e^{-\rho}, \quad Q_0(\theta) = \theta, \quad (2.2)$$

$$\kappa = +1 : \quad S_1(\rho) = \cosh \rho, \quad Q_1(\theta) = \sin \theta, \quad (2.3)$$

$$\kappa = -1 : \quad S_{-1}(\rho) = \sinh \rho, \quad Q_{-1}(\theta) = \sinh \theta, \quad (2.4)$$

with the ranges of the coordinates on dS_3 given by

$$\kappa = 0 : \quad -\infty < \rho < \infty, \quad 0 \leq \theta < \infty, \quad 0 \leq \phi < 2\pi, \quad (2.5)$$

$$\kappa = +1 : \quad -\infty < \rho < \infty, \quad 0 \leq \theta < 2\pi, \quad 0 \leq \phi < 2\pi, \quad (2.6)$$

$$\kappa = -1 : \quad 0 < \rho < \infty, \quad 0 \leq \theta < \infty, \quad 0 \leq \phi < 2\pi. \quad (2.7)$$

²While we could consider other spaces that are Weyl transforms of Minkowski spacetime as the starting point (see e.g. Ref. [13]), $dS_3 \times \mathbb{R}$ yields the three boost-invariant solutions of interest to this paper.

The three-dimensional isometry groups that correspond to the (θ, ϕ) slices for $\kappa = 0, +1, -1$ are ISO(2), SO(3) and SO(2,1), respectively. Note that, locally, the SO(2,1) slicing is an analytic continuation of the spherical SO(3) foliation. Arriving at the flat slicing from, e.g., the closed spherical slicing, requires a combination of operator rescalings and a limit, or, in the algebraic language, an operation called the group contraction.

An ideal conformal fluid in its rest frame that preserves the isometries of the slicings has the energy-momentum tensor

$$\hat{T}_{(\kappa)}^{\mu\nu} = (\hat{\varepsilon}_\kappa(\rho) + \hat{p}_\kappa(\rho)) \hat{u}^\mu \hat{u}^\nu + \hat{p}_\kappa(\rho) \hat{g}^{\mu\nu}, \quad (2.8)$$

with the velocity field $\hat{u}^\mu = (1, 0, 0, 0)$ and the equation of state $\hat{p}_\kappa = \hat{\varepsilon}_\kappa/3$. Solving the equations of motion (the energy-momentum tensor conservation or the Ward identity),

$$\hat{\nabla}_\mu \hat{T}_{(\kappa)}^{\mu\nu} = 0, \quad (2.9)$$

then gives the ρ -dependent energy densities that correspond to the three solutions:

$$\hat{\varepsilon}_0(\rho) = \mathcal{C}_0 e^{8\rho/3}, \quad \hat{\varepsilon}_{+1}(\rho) = \frac{\mathcal{C}_{+1}}{\cosh^{8/3} \rho}, \quad \hat{\varepsilon}_{-1}(\rho) = \frac{\mathcal{C}_{-1}}{\sinh^{8/3} \rho}, \quad (2.10)$$

each with an integration constant \mathcal{C}_κ . All other thermodynamic scalars of this conformal (scale-free) solution can be easily worked out by using thermodynamic identities and dimensional analysis. Note that for $\kappa = \{0, +1, -1\}$, $\hat{\nabla}_\mu \hat{u}^\mu = \{-2, 2 \tanh \rho, 2 \coth \rho\}$. Hence, for $\kappa = +1$, $-2 < \hat{\nabla}_\mu \hat{u}^\mu < 2$, and for $\kappa = -1$, $\hat{\nabla}_\mu \hat{u}^\mu > 2$.

2.2 Ideal hydrodynamic solutions in the physical (Minkowski) space

To find the corresponding conformal boost-invariant flows in the physical, flat Minkowski space expressed in terms of the Milne coordinates, we perform the Weyl transformation:

$$ds^2 = -d\tau^2 + dr^2 + r^2 d\phi^2 + \tau^2 d\eta^2 = \tau^2 d\hat{s}_\kappa^2, \quad (2.11)$$

and use the following coordinate transformations:

$$\kappa = 0 : \quad e^\rho = \tau, \quad \theta = r, \quad (2.12)$$

$$\kappa = +1 : \quad \sinh \rho = -\frac{1 - q^2 (\tau^2 - r^2)}{2q\tau}, \quad \tan \theta = \frac{2qr}{1 + q^2 (\tau^2 - r^2)}, \quad (2.13)$$

$$\kappa = -1 : \quad \cosh \rho = \frac{1 + q^2 (\tau^2 - r^2)}{2q\tau}, \quad \tanh \theta = -\frac{2qr}{1 - q^2 (\tau^2 - r^2)}, \quad (2.14)$$

where q is a free non-negative parameter. Note that in flat space, the operators of the SO(3) (the standard Gubser flow case) and SO(2,1) algebras that fix the velocity field depend on this parameter. We could therefore also call them SO(3) $_q$ and SO(2,1) $_q$. In the three cases, the allowed ranges of the flat space coordinates are $0 < r < \infty$ for the coordinate perpendicular to the beam, $0 \leq \phi < 2\pi$ for the angle in the plane transverse to the beam, $-\infty < \eta < \infty$ along the beam, and for the proper time,

$$\kappa = 0 : \quad 0 < \tau < \infty, \quad (2.15)$$

$$\kappa = +1 : \quad 0 < \tau < \infty, \quad (2.16)$$

$$\kappa = -1 : \quad \frac{1}{q^2} < \tau^2 - r^2. \quad (2.17)$$

Importantly, the $\kappa = -1$ solution can only exist within the future lightcone originating at $r = 0$, $\tau = 1/q$. The physical energy densities of the three flows are then

$$\varepsilon_0(\tau) = \frac{\mathcal{C}_0}{\tau^{4/3}}, \quad (2.18)$$

$$\varepsilon_{+1}(\tau, r) = \frac{(2q)^{8/3}\mathcal{C}_{+1}}{\tau^{4/3} [1 + 2q^2(\tau^2 + r^2) + q^4(\tau^2 - r^2)^2]^{4/3}}, \quad (2.19)$$

$$\varepsilon_{-1}(\tau, r) = \frac{(2q)^{8/3}\mathcal{C}_{-1}}{\tau^{4/3} [1 - 2q^2(\tau^2 + r^2) + q^4(\tau^2 - r^2)^2]^{4/3}}. \quad (2.20)$$

The three flows correspond to the Bjorken flow ($\kappa = 0$), the Gubser flow ($\kappa = +1$) and a new solution with $\kappa = -1$. In compact notation, the three energy densities can be written (with the numerator constants absorbed into the constant \mathcal{E}) as

$$\varepsilon_\kappa(\tau, r) = \frac{\mathcal{E}_\kappa}{\tau^{4/3} [1 + 2\kappa q^2(\tau^2 + r^2) + \kappa^2 q^4(\tau^2 - r^2)^2]^{4/3}}. \quad (2.21)$$

The four-velocity u^μ in Minkowski space is computed by using $u_\mu = \tau \hat{u}_\nu \partial \hat{x}^\nu / \partial x^\mu$. In a similarly unified notation, for all three κ ,

$$u^\tau = \frac{\kappa^2 q^2 (\tau^2 + r^2) + \kappa + (1 - \kappa)(1 + \kappa)}{\sqrt{1 + 2\kappa q^2 (\tau^2 + r^2) + \kappa^2 q^4 (\tau^2 - r^2)^2}}, \quad (2.22)$$

$$u^r = \frac{2\kappa^2 q^2 \tau r}{\sqrt{1 + 2\kappa q^2 (\tau^2 + r^2) + \kappa^2 q^4 (\tau^2 - r^2)^2}}, \quad (2.23)$$

$$u^\phi = u^\eta = 0. \quad (2.24)$$

It is easy to check that $u^\mu u_\mu = -1$. Finally, we can also compute the transverse velocity:

$$v_\perp = \frac{u^r}{u^\tau} = \frac{2\kappa^2 q^2 \tau r}{\kappa^2 q^2 (\tau^2 + r^2) + \kappa + (1 - \kappa)(1 + \kappa)}. \quad (2.25)$$

It is important to note that the hyperbolic solution has singularities at $r^2 = (\tau + 1/q)^2$ and $r^2 = (\tau - 1/q)^2$, of which only the latter lies within the coordinate range (2.17). In fact, the singularity runs along the entire edge of the lightcone, $r = \tau - 1/q$, where both the ideal energy density and the velocity field diverge.

2.3 Viscous corrections

Next, let us add the viscous corrections to the flows. For a conformal fluid, the only first-order hydrodynamic contribution arises due to the shear viscosity $\eta = H_0 \varepsilon^{3/4}$, where H_0 is a constant. In the auxiliary $dS_3 \times \mathbb{R}$, we change the energy-momentum tensor (2.8) to become

$$\hat{T}_{(\kappa)}^{\mu\nu} = (\hat{\varepsilon}_\kappa(\rho) + \hat{p}_\kappa(\rho)) \hat{u}^\mu \hat{u}^\nu + \hat{p}_\kappa(\rho) \hat{g}^{\mu\nu} - 2H_0 \hat{\varepsilon}_\kappa^{3/4}(\rho) \hat{\sigma}^{\mu\nu}, \quad (2.26)$$

where $\hat{\sigma}^{\mu\nu}$ is the standard symmetric, transverse and traceless tensor made of a single (covariant) derivative $\hat{\nabla}_\nu$ of \hat{u}^μ (see Refs. [11, 18, 19]). By the symmetry constraints, the velocity flow remains unchanged. The relativistic Navier-Stokes equations (2.9) are

then solved by incorporating the dissipative viscous correction into the energy density, or, more conveniently, the temperature field, where $\hat{\varepsilon}_\kappa = \hat{T}_\kappa^4$. Finally, by Weyl and coordinate transforming to flat spacetime, we obtain the solution for the Bjorken flow ($\kappa = 0$),

$$T_0(\tau) = \frac{\mathcal{T}_0}{\tau^{1/3}} - \frac{H_0}{2\tau}, \quad (2.27)$$

as well as for the Gubser flow ($\kappa = +1$),

$$T_{+1}(\tau, r) = \frac{1}{\tau(g^2 + 1)^{1/3}} \left[\mathcal{T}_{+1} - \frac{H_0 g^3}{9} {}_2F_1 \left(\frac{3}{2}, \frac{7}{6}; \frac{5}{2}; -g^2 \right) \right], \quad (2.28)$$

with

$$g = \frac{1 - q^2(\tau^2 - r^2)}{2q\tau}. \quad (2.29)$$

Finally, the viscous temperature field of the new solution with $\kappa = -1$ is given by³

$$T_{-1}(\tau, r) = \frac{1}{\tau(h^2 - 1)^{1/3}} \left[\mathcal{T}_{-1} - \frac{H_0 h^3}{(h^2 - 1)^{1/6}} {}_2F_1 \left(\frac{4}{3}, 1; \frac{5}{6}; -(h^2 - 1) \right) \right], \quad (2.30)$$

where

$$h = \frac{1 + q^2(\tau^2 - r^2)}{2q\tau}. \quad (2.31)$$

In all three cases, \mathcal{T}_κ are arbitrary constants.

3 Discussion of the flow solutions and future directions

I now discuss the qualitative phenomenological differences between the three boost-invariant flat-space solutions constructed in Section 2.

The Bjorken flow with $\kappa = 0$ has a constant velocity field $u^\mu = (1, 0, 0, 0)$, which implies an absence of any transverse evolution. For small τ , T_0 may become negative, making the solution unphysical. This occurs at $\tau = (H_0/2\mathcal{T}_0)^{3/2}$. We can also introduce a measure that tests the validity of the gradient expansion, i.e., a ‘Knudsen’-like number, $|\partial_\tau \ln T_0|/T_0$. It varies rapidly and has cusps for small τ . This is in the regime where the temperature can also be negative. Hence, the Bjorken flow is a good dissipative hydrodynamic solution in the regime of large τ , consistent with typical hydrodynamic expectations (despite the fact that $\tau \rightarrow \infty$ takes $T_0 \rightarrow 0$). Since this flow has been thoroughly studied in the literature, I will now mostly focus on comparing the other two solutions.

I first compare the velocity field of the Gubser flow with the $\kappa = -1$ solution. A typical situation is depicted in Figure 1. The main difference is that the Gubser flow solution is smooth and exists everywhere along the transverse plane whereas the $\kappa = -1$ solution has a sharp cutoff at the edge of the causal cone where the velocity field diverges. While the Gubser flow’s magnitude of the velocity also increases near the lightcone, this rise is gradual and smooth. One implication is therefore that far from the beam, the new solution

³Note that among many ways of writing the viscous term, we can also use the following identity: $h^3 {}_2F_1 \left(\frac{4}{3}, 1; \frac{5}{6}; -(h^2 - 1) \right) = {}_2F_1 \left(-\frac{1}{2}, -\frac{1}{6}; \frac{5}{6}; -(h^2 - 1) \right)$.

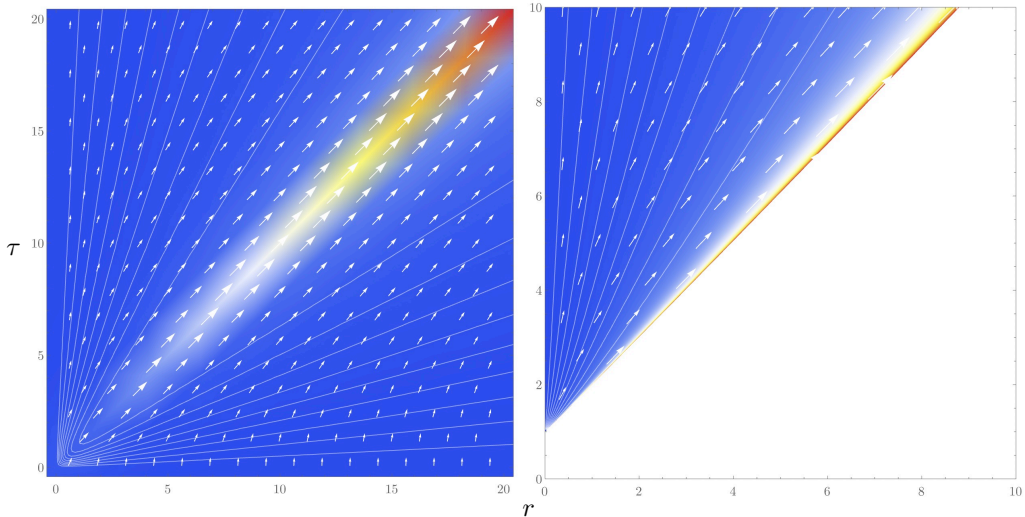


Figure 1: Velocity vector (u^r, u^τ) of the Gubser's $\kappa = +1$ (**left panel**) and the $\kappa = -1$ (**right panel**) solutions shown in the (r, τ) plane. Colours indicate the norm of the velocity vector, with its magnitude increasing from blue to red. White arrows show the size and the direction of u^μ . White lines show contours of equal transverse v_\perp , running from 0 to 1 in steps of 0.1. For the Gubser flow ($\kappa = +1$), $q = 2$, and for the $\kappa = -1$ flow, $q = 1$. The latter solution exists inside the $r < \tau - 1/q$ future lightcone, with u^μ diverging at the edge.

approaches free streaming of (massless, conformal) relativistic particles traveling at the speed of light, and behaves as a smooth shockwave. In both cases, the free parameter q effectively sets the size of the droplet. In Gubser's everywhere-smooth solution, it sets the approximate scale of its size, whereas for $\kappa = -1$, it sets the sharp edge of the lightcone where the solution ends in a divergence. As a result, the radial expansion of the droplet that follows a 'collision' of nuclei starts at the value of the proper time set by q , at $\tau = 1/q$.

Differences between the two solutions can also be seen from the radial profiles of the temperature fields $T_{\pm 1}$. This is shown in Figure 2. Focusing on the ideal limit ($H_0 = 0$), the Gubser flow is smooth for all r with the magnitude of the peak decreasing with τ . When viscosity is non-zero, however, the solution develops unphysical regions with $T_1 < 0$ for large r at early proper time. This is unlike in the $\kappa = -1$ solution, which is confined to the lightcone. There, at $H_0 = 0$, the temperature simply diverges at the lightcone. Then, as the viscosity is turned on, this divergence is smoothed and its effect is to invalidate the solution near the lightcone by making $T_{-1} < 0$, where one could imagine cutting off the solution. In fact, the region around $T_{-1} \approx 0$, near the edge of the lightcone, is the natural place to introduce a surface on which to impose freeze-out conditions. Away from the near-lightcone region, the temperature field is positive and smooth for all r and τ , even at early times. This is unlike the Gubser flow which cannot be naturally cut off at a finite r . That solution extends to infinity in perpendicular directions to the beam, for all τ .

Another important difference between the viscous flows arises in the large- τ regime. A simple way to see this and to anticipate potential pathologies is by expanding the three

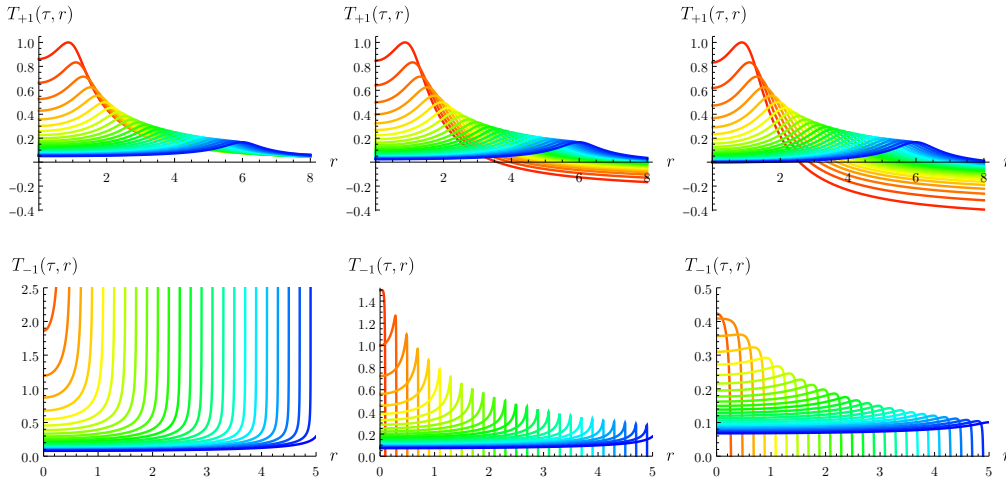


Figure 2: Evolution of the radial temperature profiles for the $\kappa = +1$ (Gubser flow) and the $\kappa = -1$ solutions. **Top:** T_{+1} from Eq. (2.28) is plotted for increasing τ from 1 (red) to 6 (blue) in spacings of 0.2. From left to right, the three plots show different values of the shear viscosity parameter $H_0 = \{0, 0.5, 1\}$, with the remaining parameters set to $\mathcal{T}_{+1} = 1$ and $q = 2$. **Bottom:** T_{-1} from Eq. (2.30), with τ running from 1.1 (red) to 6.1 (blue) in spacings of 0.2. From left to right, $H_0 = \{0, 0.3, 0.5\}$, with $\mathcal{T}_{-1} = 1$ and $q = 1$.

temperature fields. To leading order in the $\tau \rightarrow \infty$ limit, the Bjorken flow is dominated by ideal hydrodynamics, $T_0 \sim \mathcal{T}_0/\tau^{1/3}$. On the other hand, the $\kappa = \pm 1$ solutions are controlled by the viscous term, $T_{\pm 1} \sim \mp H_0/2\tau$. This makes it clear that the dominant term of the Gubser flow is negative, thereby implying a large- τ pathology. The $\kappa = -1$ solution, however, retains a positive decaying temperature as $\tau \rightarrow \infty$. Moreover, the Gubser flow solution only has small gradients for intermediate proper time scales, not at late τ . On the other hand, the $\kappa = -1$ solution retains small temperature gradients for late τ , so long as it is probed away from the null boundaries of the lightcone. This is because the energy gets accumulated near the lightcone, which allows for the relaxation of the flow everywhere inside the droplet. It is important to note, however, that despite the temperature having small and well-behaved derivatives for $\tau \gg 1$, the eventual dominance of the viscous term over the ideal term as $\tau \rightarrow \infty$ means that, strictly, the $\kappa = -1$ solution also violates the order-by-order gradient expansion. That this can happen is not particularly surprising as, indeed, all three boost-invariant flows discussed here are solutions of the fully non-linear viscous Navier-Stokes equations. I show the behaviour of the derivatives of the temperature field by plotting two representative examples of another ‘Knudsen’-like number defined in the units of the ‘curvature parameter’ q , $\tilde{K}_{\pm 1} \equiv (1/q)\sqrt{(\partial_\tau \ln T_{\pm 1})^2 + (\partial_r \ln T_{\pm 1})^2}$. The flows can be considered to be ‘well-behaved’ for $\tilde{K}_{\pm} \lesssim 1$.

In summary, the new $\kappa = -1$ solution should be phenomenologically interpreted as describing a relativistic conformal droplet confined to the future lightcone, which, as it propagates radially outwards from the beam, behaves as a free-streaming-like state at its causal edge. Similarly to the Gubser flow, the solution is boost-invariant (along the beam)

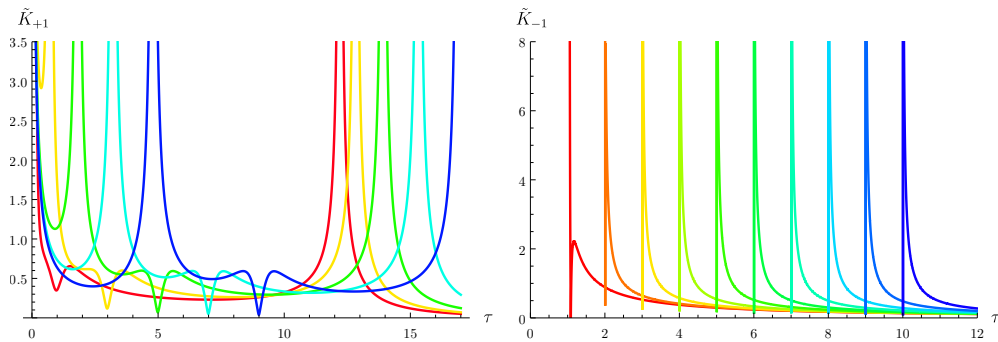


Figure 3: Plots of $\tilde{K}_{\pm 1}$ that quantifies the behaviour of the temperature gradients. **Left:** Gubser’s $\kappa = +1$ solution with $\mathcal{T}_{+1} = 1$, $q = 2$ and $H_0 = 0.5$, plotted as a function of τ , for r running from 1 (red) to 9 (blue) in steps of 2. **Right:** The $\kappa = -1$ solution with $\mathcal{T}_{-1} = 1$, $q = 1$ and $H_0 = 0.3$, shown for r between 0 (red) to 9 (blue) in steps of 1.

and radially expanding. On the other hand, what is very different from the Gubser flow is that the solution exhibits a shockwave-like expansion at the lightcone. Rather speculatively, such behaviour suggests potential relevance of the solution for the phenomenology of the colour-glass condensate and the glasma, perhaps in connection with their nearly free-streaming early-time dynamics (see Refs. [20, 21] and also Ref. [22]). Less speculatively, the $\kappa = -1$ solution may also provide a causal, boost-invariant model of a finite plasma droplet that describes the transition from hydrodynamic to ballistic expansion in heavy-ion collisions.⁴ While, as is usual with such solutions, the flow is outside of the validity of the hydrodynamic approximation at the earliest, far-from-equilibrium stage of the evolution, it should offer a realistic analytic framework for studying late-time transverse dynamics, freeze-out conditions, and for benchmarking numerical hydrodynamic simulations with finite spatial support. Therefore, this solution may naturally apply to the intermediate and late- τ regimes of a rapidly expanding quark-gluon plasma, as it retains small gradients (for any fixed r away from the causal edge of the null lightcone) and thus remains at least approximately consistent with the assumptions of the hydrodynamic derivative expansion. In this sense, the new solution combines the radial expansion characteristic of the Gubser flow with the late- τ applicability of Bjorken’s solution, while introducing the novel feature of a droplet with finite radial extent whose boundary expands in a manner reminiscent of a free-streaming shockwave.

Future studies should examine the solution more closely from the points of view of the Müller-Israel-Stewart theory and the Boltzmann equation, following, e.g., the past works in Refs. [18, 25–28], as well as with the help of the AdS/CFT correspondence, following Refs. [29–32]. With further insights drawn from all of these perspectives, we should then be able to understand the potential for applying the $\kappa = -1$ solution to the phenomenological description of realistic high-energy processes, in particular, to the collisions of heavy ions, and the formation of quark-gluon plasma.

⁴For an intriguing hydrodynamic–ballistic matching in unitary Fermi gases, see Refs. [23, 24].

Acknowledgments

I would like to thank Mauricio Martinez, Wilke van der Schee and Alexander Soloviev for helpful and stimulating discussions. This work was supported by the STFC Ernest Rutherford Fellowship ST/T00388X/1. It was also supported by the research programme P1-0402 and the project J7-60121 of Slovenian Research Agency (ARIS).

References

- [1] L. Landau and E. Lifshits, *Fluid Mechanics*. Pergamon Press, New York, 1987.
- [2] P. Kovtun, *Lectures on hydrodynamic fluctuations in relativistic theories*, *J. Phys.* **A45** (2012) 473001 [[1205.5040](#)].
- [3] P. Romatschke and U. Romatschke, *Relativistic Fluid Dynamics In and Out of Equilibrium*, Cambridge Monographs on Mathematical Physics. Cambridge University Press, 5, 2019, [10.1017/9781108651998](#), [[1712.05815](#)].
- [4] W. Busza, K. Rajagopal and W. van der Schee, *Heavy Ion Collisions: The Big Picture, and the Big Questions*, *Ann. Rev. Nucl. Part. Sci.* **68** (2018) 339 [[1802.04801](#)].
- [5] P. M. Chesler and L. G. Yaffe, *Numerical solution of gravitational dynamics in asymptotically anti-de Sitter spacetimes*, *JHEP* **07** (2014) 086 [[1309.1439](#)].
- [6] W. van der Schee, P. Romatschke and S. Pratt, *Fully Dynamical Simulation of Central Nuclear Collisions*, *Phys. Rev. Lett.* **111** (2013) 222302 [[1307.2539](#)].
- [7] M. P. Heller, *Holography, Hydrodynamization and Heavy-Ion Collisions*, *Acta Phys. Polon. B* **47** (2016) 2581 [[1610.02023](#)].
- [8] S. Grozdanov and W. van der Schee, *Coupling Constant Corrections in a Holographic Model of Heavy Ion Collisions*, *Phys. Rev. Lett.* **119** (2017) 011601 [[1610.08976](#)].
- [9] J. D. Bjorken, *Highly Relativistic Nucleus-Nucleus Collisions: The Central Rapidity Region*, *Phys. Rev.* **D27** (1983) 140.
- [10] S. S. Gubser, *Symmetry constraints on generalizations of Bjorken flow*, *Phys. Rev. D* **82** (2010) 085027 [[1006.0006](#)].
- [11] S. S. Gubser and A. Yarom, *Conformal hydrodynamics in Minkowski and de Sitter spacetimes*, *Nucl. Phys. B* **846** (2011) 469 [[1012.1314](#)].
- [12] Y. Hatta, J. Noronha and B.-W. Xiao, *Exact analytical solutions of second-order conformal hydrodynamics*, *Phys. Rev. D* **89** (2014) 051702 [[1401.6248](#)].
- [13] Y. Hatta, J. Noronha and B.-W. Xiao, *A systematic study of exact solutions in second-order conformal hydrodynamics*, *Phys. Rev. D* **89** (2014) 114011 [[1403.7693](#)].
- [14] M. I. Nagy, T. Csorgo and M. Csanad, *Detailed description of accelerating, simple solutions of relativistic perfect fluid hydrodynamics*, *Phys. Rev. C* **77** (2008) 024908 [[0709.3677](#)].
- [15] M. I. Nagy, *New simple explicit solutions of perfect fluid hydrodynamics and phase-space evolution*, *Phys. Rev. C* **83** (2011) 054901 [[0909.4285](#)].
- [16] H. Bantilan, T. Ishii and P. Romatschke, *Holographic Heavy-Ion Collisions: Analytic Solutions with Longitudinal Flow, Elliptic Flow and Vorticity*, *Phys. Lett. B* **785** (2018) 201 [[1803.10774](#)].

- [17] T. Csörgő, G. Kasza, M. Csanád and Z. Jiang, *New exact solutions of relativistic hydrodynamics for longitudinally expanding fireballs*, *Universe* **4** (2018) 69 [1805.01427].
- [18] R. Baier, P. Romatschke, D. T. Son, A. O. Starinets and M. A. Stephanov, *Relativistic viscous hydrodynamics, conformal invariance, and holography*, *JHEP* **04** (2008) 100 [0712.2451].
- [19] S. Grozdanov and N. Kaplis, *Constructing higher-order hydrodynamics: The third order*, *Phys. Rev.* **D93** (2016) 066012 [1507.02461].
- [20] E. Iancu and R. Venugopalan, *The Color glass condensate and high-energy scattering in QCD*. [hep-ph/0303204](#).
- [21] F. Gelis, *Color Glass Condensate and Glasma*, *Int. J. Mod. Phys. A* **28** (2013) 1330001 [1211.3327].
- [22] S. S. Gubser, *Complex deformations of Bjorken flow*, *Phys. Rev. C* **87** (2013) 014909 [1210.4181].
- [23] M. Bluhm and T. Schaefer, *Model-independent determination of the shear viscosity of a trapped unitary Fermi gas: Application to high temperature data*, *Phys. Rev. Lett.* **116** (2016) 115301 [1512.00862].
- [24] M. Bluhm, J. Hou and T. Schäfer, *Determination of the density and temperature dependence of the shear viscosity of a unitary Fermi gas based on hydrodynamic flow*, *Phys. Rev. Lett.* **119** (2017) 065302 [1704.03720].
- [25] F. S. Bemfica, M. M. Disconzi and J. Noronha, *Causality and existence of solutions of relativistic viscous fluid dynamics with gravity*, *Phys. Rev. D* **98** (2018) 104064 [1708.06255].
- [26] G. S. Denicol, U. W. Heinz, M. Martinez, J. Noronha and M. Strickland, *Studying the validity of relativistic hydrodynamics with a new exact solution of the Boltzmann equation*, *Phys. Rev. D* **90** (2014) 125026 [1408.7048].
- [27] M. Nopoush, R. Ryblewski and M. Strickland, *Anisotropic hydrodynamics for conformal Gubser flow*, *Phys. Rev. D* **91** (2015) 045007 [1410.6790].
- [28] M. Martinez, M. McNelis and U. Heinz, *Anisotropic fluid dynamics for Gubser flow*, *Phys. Rev. C* **95** (2017) 054907 [1703.10955].
- [29] R. A. Janik and R. B. Peschanski, *Asymptotic perfect fluid dynamics as a consequence of AdS/CFT*, *Phys. Rev. D* **73** (2006) 045013 [hep-th/0512162].
- [30] R. A. Janik, *Viscous plasma evolution from gravity using AdS/CFT*, *Phys. Rev. Lett.* **98** (2007) 022302 [hep-th/0610144].
- [31] A. Banerjee, T. Mitra, A. Mukhopadhyay and A. Soloviev, *How Gubser flow ends in a holographic conformal theory*, *Eur. Phys. J. C* **84** (2024) 550 [2307.10384].
- [32] T. Mitra, S. Mondkar, A. Mukhopadhyay and A. Soloviev, *Holographic Gubser flow. A combined analytic and numerical study*, *JHEP* **10** (2024) 226 [2408.04001].